Optical and electronic properties in $(In_{0.53}Ga_{0.47}As)_{1-z}/(In_{0.52}Al_{0.48}As)_z$ digital alloys

J. T. Woo, J. H. Kim, and T. W. Kim*
Research Institute of Information Display, Division of Electronics and Computer Engineering, Hanyang University, 17 Haengdang-dong, Seongdong-gu, Seoul 133-791, Korea

J. D. Song and Y. J. Park
Nanodevice Research Center, Korea Institute of Science and Technology, Seoul 136-791, Korea
(Received 12 April 2005; revised manuscript received 22 August 2005; published 11 November 2005)

The optical and electronic properties in $(In_{0.53}Ga_{0.47}As)_{1-z}/(In_{0.52}Al_{0.48}As)_z$ digital alloys with various compositions grown on InP substrates by using molecular-beam epitaxy were investigated through photoluminescence (PL) measurements and numerical calculations. The electronic subband energy states, the interband transition energies, and the exciton binding energies of $(In_{0.53}Ga_{0.47}As)_{1-z}/(In_{0.52}Al_{0.48}As)_z$ digital alloys and corresponding $In_{0.53}Ga_{0.47}As/In_{0.52}Al_{0.48}As$ single quantum wells were calculated by using a finite difference method, taking into account two band Hamiltonian system. The numerical results for interband transitions of $(In_{0.53}Ga_{0.47}As)_{1-z}/(In_{0.52}Al_{0.48}As)_z$ digital alloys were in reasonable agreement with the excitonic transitions obtained from the PL measurements.

DOI: 10.1103/PhysRevB.72.205320 PACS number(s): 73.21.Cd, 78.55.Cr

I. INTRODUCTION

Digital alloy structures are particularly attractive because of their potential applications in optoelectronic devices, such as light emitters and Bragg reflector mirrors.[1] In particular, the $(In_{0.53}Ga_{0.47}As)_{1-z}/(In_{0.52}Al_{0.48}As)_z$ digital alloys have been very important for applications in lattice-matched multiquantum well (MQW) laser diodes,[2] broadband-emission triple-quantum-well light-emitting diodes,[3] strained MQW lasers,[4,5] vertical cavity surface emitting lasers,[6] and avalanche photodiodes[7] operating at 1.55 μm. When the relative thicknesses of the two heterointerfaces and the compositions of the unit quantum well structure are precisely controlled, the digital alloy technique overcomes inherent problems encountered in the conventional molecular beam epitaxy (MBE), such as the requirements for the additional source cells and for rapid changes of the effusion cell flux and of the cell temperature during growth interruption.[2] Even though some works concerning the growth and the physical properties of the $(Al_xGa_{1-x}As)_1/(GaAs)_m$ and the $(In_xGa_{1-x}As)_{1-z}/(In_yAl_{1-y}As)_z$ digital alloys have been reported,[8,9] systematic studies on the optical and the electronic properties of $(In_{0.53}Ga_{0.47}As)_{1-z}/(In_{0.52}Al_{0.48}As)_z$ digital alloys have not yet been performed because of the delicate problems encountered in the growth process.

This paper reported on the optical and the electronic properties of lattice-matched $(In_{0.53}Ga_{0.47}As)_{1-z}/(In_{0.52}Al_{0.48}As)_z$ digital alloys grown by using MBE. Photoluminescence (PL) measurements were performed in order to investigate the optical properties of the $(In_{0.53}Ga_{0.47}As)_{1-z}/(In_{0.52}Al_{0.48}As)_z$ digital alloys, and the electronic subband energies and the wave functions in the digital alloys and the single quantum wells corresponding to each other digital alloy structures were calculated by using a finite difference method and taking into account two-band Hamiltonian systems considering a conduction band and a heavy-hole band. The interband transition energies of the $(In_{0.53}Ga_{0.47}As)_{1-z}/(In_{0.52}Al_{0.48}As)_z$ digital alloys at different temperatures were compared with those of the $In_{0.53}Ga_{0.47}As/In_{0.52}Al_{0.48}As$ single quantum well. Furthermore, the exciton binding energies in the $(In_{0.53}Ga_{0.47}As)_{1-z}/(In_{0.52}Al_{0.48}As)_z$ digital alloys were described as a function of the unit well width.

II. EXPERIMENTAL DETAILS

The several kinds of lattice-matched $(In_{0.53}Ga_{0.47}As)_{1-z}/(In_{0.52}Al_{0.48}As)_z$ digital alloys were grown on InP substrates by using MBE. After the InP substrates had been cleaned chemically, a 1000 Å thick $In_{0.52}Al_{0.48}As$ cladding layer was deposited at a growth temperature of 510 °C. Lattice-matched $(In_{0.53}Ga_{0.47}As)_{1-z}/(In_{0.52}Al_{0.48}As)_z$ digital alloys with z compositions of 0.2, 0.4, 0.6, or 0.8 were grown under the same growth conditions, keeping the period of the $(In_{0.53}Ga_{0.47}As)_{1-z}/(In_{0.52}Al_{0.48}As)_z$ digital alloys at between 16 and 19 Å thickness. Finally, a 250 Å thick $In_{0.52}Al_{0.48}As$ capping layer was grown on a 1000 Å thick $In_{0.52}Al_{0.48}As$ cladding layer. The concentrations of In, Ga, and Al in the $(In_xGa_{1-x}As)_{1-z}/(In_yAl_{1-y}As)_z$ digital alloys are determined by using double-crystal x-ray diffraction measurements. A detailed growth procedure for the digital alloy $(In_{0.53}Ga_{0.47}As)_{1-z}/(In_{0.52}Al_{0.48}As)_z$ was reported elsewhere.[9] The growth rates of $In_{0.53}Ga_{0.47}As$ and $In_{0.52}Al_{0.48}As$ were 0.929 μm/h. Schematic diagrams of the structure and of the corresponding unit structures of the digital alloy samples are shown in Figs. 1(a) and 1(b), respectively.

PL measurements were performed by using an 1 m monochromator equipped with RCA 31034 photomultiplier tube. The excitation source was the 514.5 nm line of an Ar^+ ion laser. The samples were mounted on a cold finger in a cryostat and kept at 9 K by using a He displex system. The laser beam was focused with a lens, and the size of the beam was 0.3 mm in diameter. The excitation power intensities were 177, 355, and 532 mW/mm^2.

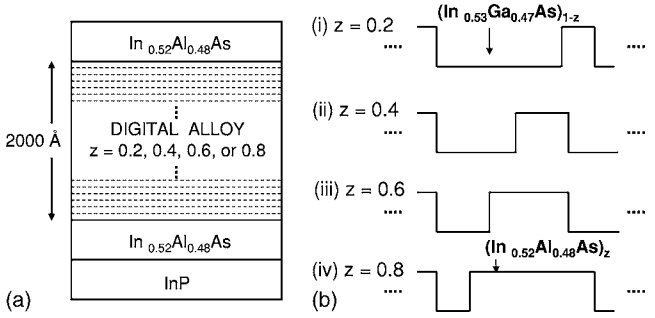

FIG. 1. (a) Schematic diagram of the $(In_{0.53}Ga_{0.47}As)_{1-z}/(In_{0.52}Al_{0.48}As)_z$ digital alloys structures and (b) electronic structures corresponding to the conduction bands of the $(In_{0.53}Ga_{0.47}As)_{1-z}/(In_{0.52}Al_{0.48}As)_z$ digital alloys structures with (i) $z=0.2$; $In_{0.53}Ga_{0.47}As$ (15 Å) and $In_{0.52}Al_{0.48}As$ (3.75 Å), (ii) $z=0.4$; $In_{0.53}Ga_{0.47}As$ (9.8 Å) and $In_{0.52}Al_{0.48}As$ (6.6 Å), (iii) $z=0.6$; $In_{0.53}Ga_{0.47}As$ (6.6 Å) and $In_{0.52}Al_{0.48}As$ (9.8 Å), and (iv) $z=0.8$; $In_{0.53}Ga_{0.47}As$ (3.75 Å) and $In_{0.52}Al_{0.48}As$ (15 Å).

III. THEORETICAL CONSIDERATION

A two-band Hamiltonian system, including the conduction band and the heavy hole band structures, is introduced to solve the eigenvalue problem by using a finite difference method (FDM). The eigenvalue problem with a very large-scale spare matrix was numerically solved by using an Arnoldi method.[10] To obtain accurate simulation results for the interband transition energies of the $(In_{0.53}Ga_{0.47}As)_{1-z}/(In_{0.52}Al_{0.48}As)_z$ digital alloys, we considered the δ-function property of the $\partial m^*(z)/\partial z$ at the abrupt potential boundary by expanding the derivative on z one more. The physical parameters used in this study to calculate the electronic states of the $(In_{0.53}Ga_{0.47}As)_{1-z}/(In_{0.52}Al_{0.48}As)_z$ digital alloys are listed in Table I. The band-gap energies of the $(In_{0.53}Ga_{0.47}As)_{1-z}/(In_{0.52}Al_{0.48}As)_z$ digital alloys were obtained by interpolating the Lagrange polynomials and taking into account the representative experimental data.[11,12]

The exciton binding energies of the $(In_{0.53}Ga_{0.47}As)_{1-z}/(In_{0.52}Al_{0.48}As)_z$ digital alloy structures were calculated by using the wave functions obtained from previous results of the eigenvalue problem on the two-band Hamiltonian system. The total Hamiltonian (H) can be expanded to be the sum of three terms, which is $H=H_e+H_h+H_{e\text{-}h}$. The first two terms on the right-hand side are the Hamiltonians of the electron in the conduction band (H_e) and the hole in the heavy hole band (H_h), respectively,

TABLE I. Physical parameters used in this study for the calculation of the electronic structures of the digital alloy $(In_{0.53}Ga_{0.47}As)_{1-z}/(In_{0.52}Al_{0.48}As)_z$ structures.

		$In_{0.53}Ga_{0.47}As$	$In_{0.52}Al_{0.48}As$
Effective mass (m_e)	Electrons	0.041	0.075
	Heavy holes	0.465	0.41
Band gap (eV)	9 K	0.8115201	1.50702
	300 K	0.75	1.45

$$H_e = -\frac{\hbar^2}{2m_e^*}\frac{\partial^2}{\partial z^2} + V_C(z), \quad H_h = -\frac{\hbar^2}{2m_h^*}\frac{\partial^2}{\partial z^2} + V_V(z). \quad (1)$$

The third term represents the Hamiltonian of the electron-hole interaction ($H_{e\text{-}h}$), which is composed of the kinetic energy term and the Coulombic potential energy term,

$$H_{e\text{-}h} = \frac{P_\perp^2}{2\mu_\perp} - \frac{e^2}{4\pi\varepsilon_r\varepsilon_0 r}, \quad P_\perp^2 = -\hbar^2\left(\frac{\partial^2}{\partial x^2} + \frac{\partial^2}{\partial y^2}\right), \quad (2)$$

where r is the distance between the electron and the hole, $\mu_\perp$ is the reduced mass calculated from the weighted averages of $m_{\perp e}$ and $m_{\perp h}$ of the effective masses, ε_r is the weighted average between dielectric constants. For the two-body exciton wave function $\Psi=\psi_e(z_e)\psi_h(z_h)\psi_r$ where ψ_e and ψ_h are wave functions of the electron and the hole along growth direction, respectively, and ψ_r represents the wave function of the electron and the hole relative motion which is a variational wave function to minimize the total energy $E=\langle\Psi|H|\Psi\rangle/\langle\Psi|\Psi\rangle$. Consequently, the exciton binding energy of the digital alloy structures can be written as the following equation:[13–15]

$$E_{X^0} = \frac{\hbar^2}{2\langle\Psi|\Psi\rangle}\left\{\int_0^N p(a)\left[\int\left(\frac{1}{m_{\perp e}}\left|\frac{\partial\psi_r}{\partial z_e}\right|^2 + \frac{1}{m_{\perp h}}\left|\frac{\partial\psi_r}{\partial z_h}\right|^2\right)dx\,dy\right]da + \langle\Psi|H_{e\text{-}h}|\Psi\rangle\right\}, \quad N \gg L, \quad (3)$$

where $p(a)$ is the uncorrelated probability of finding the electron and hole within a distance a, and L is the thickness of the digital alloy structure. In this approach, effective masses and dielectric constants of the digital alloy structures are determined by their average values, considering their contributions on the overall structures.

IV. RESULTS AND DISCUSSION

Figure 2 shows PL spectra for the $(In_{0.53}Ga_{0.47}As)_{0.6}/(In_{0.52}Al_{0.48}As)_{0.4}$ digital alloys measured at various excitation power intensities. The PL spectrum shape was insensitive to the excitation power intensities of the laser from 177 to 532 mW/mm^2 as shown in Fig. 2, and the intensity of PL spectrum linearly increased with increasing excitation power intensity. The results of the PL measurements were not significantly affected by a high carrier density in the sample, and the PL spectra do not show any band filling effect. Figure 3 shows PL spectra measured at 9 K for $(In_{0.53}Ga_{0.47}As)_{1-z}/(In_{0.52}Al_{0.48}As)_z$ digital alloys with various z compositions. The dominant excitonic peak shifted to the higher energy side with increasing z composition.

Figure 4 shows a convergence of the theoretical interband transition energies of the $(In_{0.53}Ga_{0.47}As)_{1-z}/(In_{0.52}Al_{0.48}As)_z$ digital alloy and the $In_{0.53}Ga_{0.47}As/In_{0.52}Al_{0.48}As$ single quantum well with respect to the unit mesh size in a FDM. Stable convergences of the numerical results for the digital alloy structures were obtained in the condition that a unit mesh size is smaller than 0.5 Å, as shown in Fig. 4. Figure 5

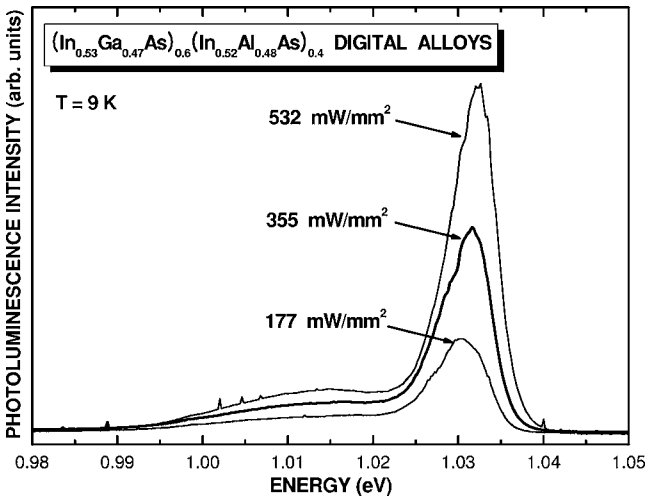

FIG. 2. Photoluminescence spectra for the $(In_{0.53}Ga_{0.47}As)_{0.6}/(In_{0.52}Al_{0.48}As)_{0.4}$ digital alloys measured at various excitation power intensities.

shows the interband transitions as a function of the z composition at 9 K for the $(In_{0.53}Ga_{0.47}As)_{1-z}/(In_{0.52}Al_{0.48}As)_z$ digital alloys with various band offsets. The deviations of the interband transition energies dependent on various band offset ratios, from 0.4 to 0.8, are always below 20 meV regardless of the values of the band offset ratio. In this study, the band offset ratio is always assumed to be 0.6.

The theoretical and the experimental interband transition energies of the $(In_{0.53}Ga_{0.47}As)_{1-z}/(In_{0.52}Al_{0.48}As)_z$ digital alloys at 9 and 300 K are in a good agreement with each other, as shown in Figs. 6(a) and 6(b), respectively. The difference between theoretical and experimental values is at most 43 meV. Although considering uncertainty caused by interdiffusion effect between heterojunctions in growth, these results show our model is appropriate to describe the interband transition between conduction band and heavy hole band in the digital alloy structures.

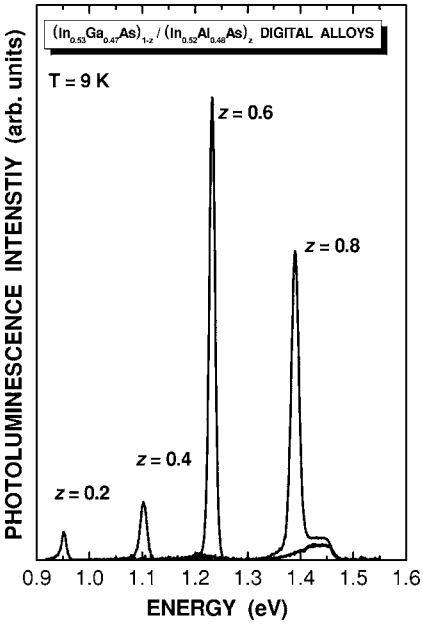

FIG. 3. Photoluminescence spectra for the $(In_{0.53}Ga_{0.47}As)_{1-z}/(In_{0.52}Al_{0.48}As)_z$ digital alloys with z values of 0.2, 0.4, 0.6, or 0.8.

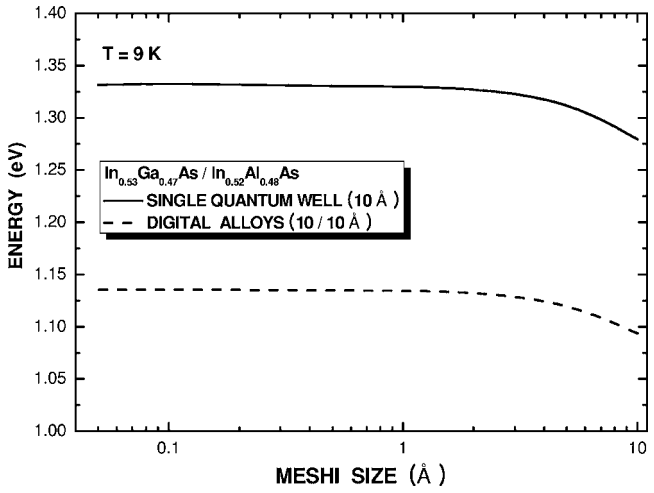

FIG. 4. The convergence of the theoretical interband transition energies with respect to the unit mesh size in a finite difference method. The solid line indicates the theoretical values for the $(In_{0.53}Ga_{0.47}As)/(In_{0.52}Al_{0.48}As)$ single quantum well (10 Å). The dashed line indicates the theoretical values for the $(In_{0.53}Ga_{0.47}As)/(In_{0.52}Al_{0.48}As)$ digital alloys (10 Å/10 Å).

Figure 7 shows a variation of the exciton binding energies of the $(In_{0.53}Ga_{0.47}As)_{1-z}/(In_{0.52}Al_{0.48}As)_z$ digital alloys and the $In_{0.53}Ga_{0.47}As/In_{0.52}Al_{0.48}As$ single quantum well corresponding to the digital alloy structures as a function of well width. There are certain points to note about these results that the exciton binding energies of the $(In_{0.53}Ga_{0.47}As)_{1-z}/(In_{0.52}Al_{0.48}As)_z$ digital alloys and the $In_{0.53}Ga_{0.47}As/In_{0.52}Al_{0.48}As$ single quantum well exhibit an opposite trend.

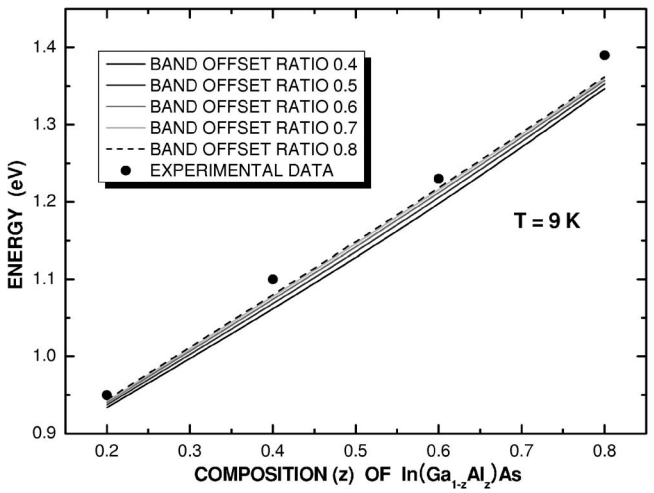

FIG. 5. The interband transitions as a function of the z composition at 9 K for the $(In_{0.53}Ga_{0.47}As)_{1-z}/(In_{0.52}Al_{0.48}As)_z$ digital alloys. The filled circles and the lines represent the experimental data and the theoretical values for the $(In_{0.53}Ga_{0.47}As)_{1-z}/(In_{0.52}Al_{0.48}As)_z$ digital alloys, respectively. Each line indicates the theoretical values obtained by using various band offset ratios, from 0.4 to 0.8.

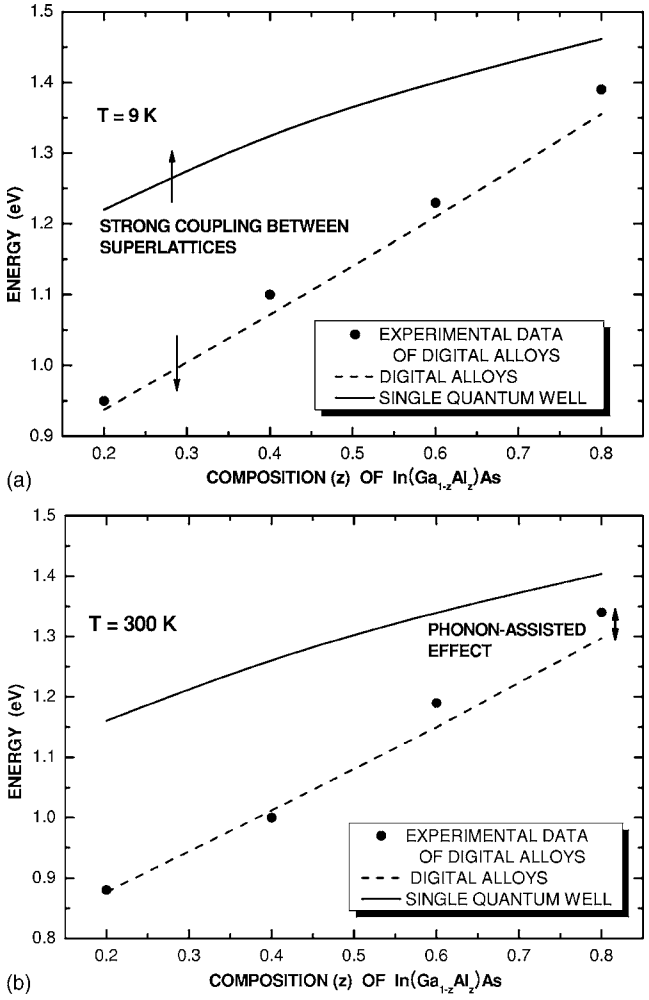

FIG. 6. The interband transitions as a function of the z composition at (a) 9 and (b) 300 K for the $(In_{0.53}Ga_{0.47}As)_{1-z}/(In_{0.52}Al_{0.48}As)_z$ digital alloys. The filled circles and the dashed line represent the experimental data and the theoretical values for the $(In_{0.53}Ga_{0.47}As)_{1-z}/(In_{0.52}Al_{0.48}As)_z$ digital alloys, respectively. The solid line indicates the theoretical values for a $In_{0.53}Ga_{0.47}As/In_{0.52}Al_{0.48}As$ single quantum well.

In the case of a single quantum well structure, as the well width decreases, the envelope function penetration into barrier remarkably increases. As a result, the effective distance of electron and hole increases and the exciton binding energy decreases. However, a description on a small increment of the exciton binding energy in the $(In_{0.53}Ga_{0.47}As)_{1-z}/(In_{0.52}Al_{0.48}As)_z$ digital alloys is not so simple, because digital alloy structure shows uncorrelated Coulombic interaction. Nevertheless, the envelope function for the $(In_{0.53}Ga_{0.47}As)_{1-z}/(In_{0.52}Al_{0.48}As)_z$ digital alloys with a z value of 0.8 is more localized in the quantum well regions in comparison with that of the digital alloy structure with a z value of 0.2 as shown in Figs. 8(a) and 8(b). Therefore, when the unit well width of the digital alloy structure decreases, a slight increase of the exciton binding energy can be explained by a local quantum confinement effect into unit well regions of the digital alloy structure.

To compare the interband transition energies of the $In_{0.53}Ga_{0.47}As/In_{0.52}Al_{0.48}As$ single quantum well structures

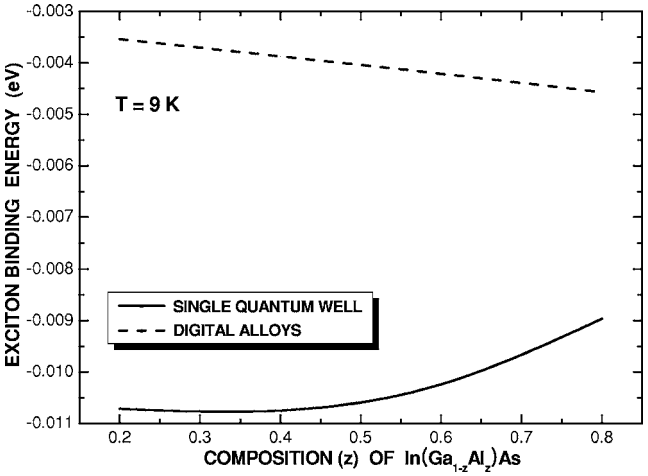

FIG. 7. Theoretical values of the exciton binding energies for the $(In_{0.53}Ga_{0.47}As)_{1-z}/(In_{0.52}Al_{0.48}As)_z$ digital alloys and the $In_{0.53}Ga_{0.47}As/In_{0.52}Al_{0.48}As$ single quantum well. The dashed line represent the $(In_{0.53}Ga_{0.47}As)_{1-z}/(In_{0.52}Al_{0.48}As)_z$ digital alloys with z values of 0.2, 0.4, 0.6, or 0.8. The solid line indicates for a $In_{0.53}Ga_{0.47}As/In_{0.52}Al_{0.48}As$ single quantum well.

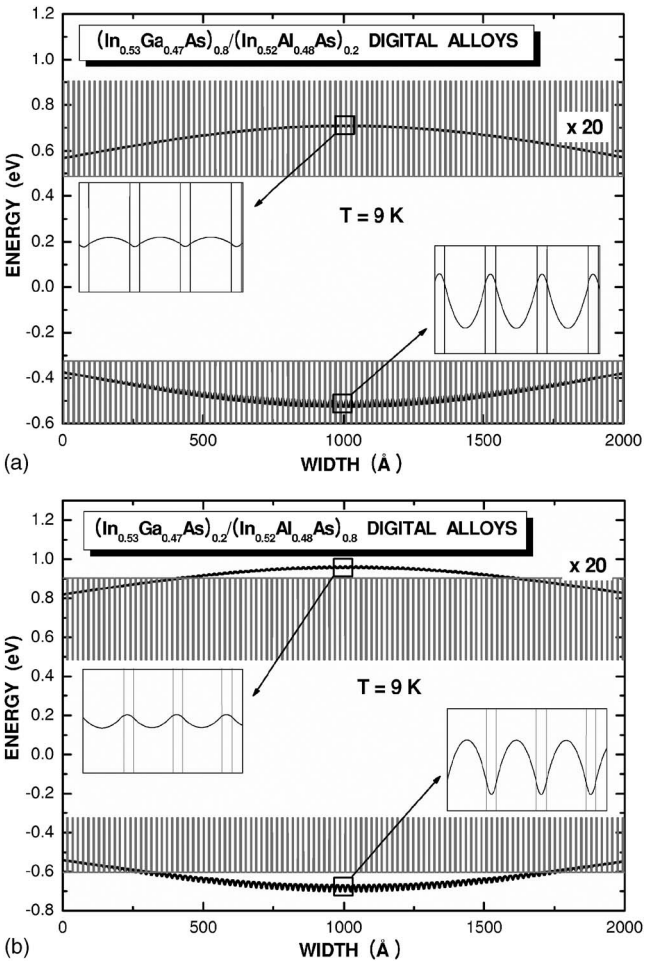

FIG. 8. Envelope functions as a function of the quantum-well width for the $(In_{0.53}Ga_{0.47}As)_{1-z}(In_{0.52}Al_{0.48}As)_z$ digital alloys structures with a z value of (a) 0.2 and (b) 0.8. The insets indicate the magnified envelope functions of the rectangular area.

with well widths of 3.75, 6.6, 9.8, and 15 Å, which are corresponding to unit structure of the $(In_{0.53}Ga_{0.47}As)_{1-z}/(In_{0.52}Al_{0.48}As)_z$ digital alloys with z compositions of 0.2, 0.4, 0.6, and 0.8, respectively, we calculated the transition energies in the $In_{0.53}Ga_{0.47}As/In_{0.52}Al_{0.48}As$ single quantum wells. The large difference in the interband transitions between the $(In_{0.53}Ga_{0.47}As)_{0.8}/(In_{0.52}Al_{0.48}As)_{0.2}$ digital alloys and the corresponding quantum well structures reflects that the interband transitions of $(In_{0.53}Ga_{0.47}As)_{1-z}/(In_{0.52}Al_{0.48}As)_z$ digital alloys structures are affected by a 1000 nm bulk digital alloy structure rather than a unit of the $In_{0.53}Ga_{0.47}As/In_{0.52}Al_{0.48}As$ single quantum well, as shown in Figs. 8(a) and 8(b). The insets in Figs. 8(a) and 8(b) give the magnified envelope functions of $(In_{0.53}Ga_{0.47}As)_{1-z}/(In_{0.52}Al_{0.48}As)_z$ digital alloys with z values of 0.2 and 0.8, respectively. While the envelope functions of the $(In_{0.53}Ga_{0.47}As)_{1-z}/(In_{0.52}Al_{0.48}As)_z$ digital alloys at $z=0.8$ are strongly localized in the single quantum well regions, those of $z=0.2$ show a weak interaction with the single quantum well structures. When the width of the $In_{0.52}Al_{0.48}As$ barriers is smaller than that of the $In_{0.53}Ga_{0.47}As$ wells, a comparison of the single quantum well and the digital alloy structures show that redshifts of transition energies become dominant.

V. SUMMARY AND CONCLUSIONS

Systematic studies on the optical and the electronic subband properties of $(In_{0.53}Ga_{0.47}As)_{1-z}/(In_{0.52}Al_{0.48}As)_z$ digital alloy structures were investigated. The interband transition energies between conduction band and heavy hole band in the $(In_{0.53}Ga_{0.47}As)_{1-z}/(In_{0.52}Al_{0.48}As)_z$ digital alloys were obtained from the PL measurements, and the results were in reasonable agreement with those determined from the theoretical calculations. The simulated values of the exciton binding energies in the $(In_{0.53}Ga_{0.47}As)_{1-z}/(In_{0.52}Al_{0.48}As)_z$ digital alloys were as small as below 4.5 meV, and the exciton binding energy slightly increases with decreasing unit well width of the digital alloy structure due to a local quantum confinement effect into unit well regions. These results indicate that the $(In_{0.53}Ga_{0.47}As)_{1-z}/(In_{0.52}Al_{0.48}As)_z$ digital alloy structures hold promise for applications in optoelectronic devices utilizing interband transitions, such as vertical-cavity surface-emitting lasers operating at 1.55 μm.

ACKNOWLEDGMENT

This work was supported by the Korea Research Foundation Grant. (KRF-2004-005-D00166)

*Corresponding author. Electronic address: twk@hanyang.ac.kr

[1] R. Kuchibhotla, J. C. Campbell, J. C. Bean, L. Peticolas, and R. Hull, Appl. Phys. Lett. **62**, 2215 (1993).
[2] G. T. Liu, A. Stintz, E. A. Pease, T. C. Newell, K. J. Malloy, and L. F. Lester, IEEE Photonics Technol. Lett. **12**, 4 (2000).
[3] I. J. Fritz, M. J. Hafich, J. F. Klem, and S. A. Casalnuovo, Electron. Lett. **35**, 171 (1999).
[4] A. J. Springthorpe, T. Garanzotis, P. Paddon, G. Pakulski, and K. I. White, Electron. Lett. **36**, 1031 (2000).
[5] M. H. M. Reddy, A. Huntington, D. Buell, R. Koda, E. Hall, and L. A. Coldren, Appl. Phys. Lett. **80**, 3509 (2002).
[6] M. H. M. Reddy, D. A. Buell, D. Feezell, T. Asano, R. Koda, A. S. Huntington, and L. A. Coldren, IEEE Photonics Technol. Lett. **15**, 891 (2003).
[7] S. Wang, J. B. Hurst, F. Ma, R. Sidhu, X. Sun, X. G. Zheng, A. L. Holmes, A. Huntington, and L. A. Coldren, IEEE Photonics Technol. Lett. **14**, 1722 (2003).
[8] D. S. Jiang, K. Kelting, T. Isu, H. J. Queisser, and K. Ploog, J. Appl. Phys. **63**, 845 (1988).
[9] J. D. Song, J. S. Yu, J. M. Kim, S. J. Bae, and Y. T. Lee, Appl. Phys. Lett. **80**, 4650 (2002).
[10] D. C. Sorensen, SIAM J. Matrix Anal. Appl. **13**, 357 (1992).
[11] S. L. Chuang, *Physics of Optoelectronic Devices* (Wiley, New York, 1995), Appendix K.
[12] *Semiconductors-Basic Data*, 2nd ed., edited by O. Madelung (Springer-Verlag, Berlin, 1996).
[13] C. P. Hilto, W. E. Hagston, and J. E. Nicholls, J. Phys. A **25**, 2395 (1992).
[14] P. Hilto, J. Goodwin, P. Harrison, and W. E. Hagston, J. Phys. A **25**, 5365 (1992).
[15] P. Harrison, J. Goodwin, and W. E. Hagston, Phys. Rev. B **46**, 12377 (1992).